

# ON THE THEORY OF FRACTURE OF CURVED SHEETS

E. S. FOLIAS†

Department of Mechanics and Applied Mathematics, College of Engineering, University of Utah,  
Salt Lake City, Utah 84112, U.S.A.

**Abstract**—Following Griffith, a fracture criterion incorporating a geometry and plasticity correction is derived for the prediction of failure in pressurized vessels. A comparison with a few sets of experimental data chosen at random is very good.

## NOTATION

- $A$  = projected area on the base plane
- $c$  = half crack length
- $c_e = c + \rho$  = half effective crack length
- $D = Eh^3/[12(1-\nu^2)]$  = flexural rigidity
- $E$  = Young's modulus
- $G$  = shear modulus
- $h$  = thickness
- $K$  = fracture toughness
- $J, I, J_{c,a}, I_{c,a}, J_s, I_s, J_{c,p}, I_{c,p}$  as defined in text
- $P$  = periphery
- $P^{(e)}, P^{(b)}, P_s^{(e)}, P_p^{(e)}, P_{c,a}^{(e)}, P_{c,p}^{(e)}, P_s^{(b)}, P_p^{(b)}, P_{c,a}^{(b)}, P_{c,p}^{(b)}$   
= stress coefficients as defined in text
- $q_0$  = uniform internal pressure
- $R$  = radius of the shell
- $r = \sqrt{x^2 + y^2}, \theta = \tan^{-1} \frac{y}{x}$
- $U$  = total energy of the system
- $U_0$  = constant or datum energy
- $x, y, z$  = rectangular cartesian coordinates
- $\gamma = 0.5768 \dots$  = Euler's constant
- $\gamma^*$  = surface energy per unit area
- $\Gamma$  = path of integration as defined in Fig. 1
- $\delta$  = as defined in text.
- $\lambda^4 = \frac{Ehc^4}{R^2D} = \frac{12(1-\nu^2)c^4}{R^2h^2}$
- $\nu$  = Poisson's ratio
- $\nu_0 = 1 - \nu$
- $\pi = 3.14$
- $\rho$  = size of plastic zone
- $\sigma$  = normal stress as defined in Fig. 3
- $\sigma_y$  = yield stress
- $\sigma_u$  = ultimate stress
- $\sigma^* = \frac{\sigma_y + (\sigma_y + \sigma_u)/2}{2}$  (see also footnote on page 156)
- $\sigma_F$  = fracture stress
- $\sigma_h$  = hoop stress
- $\sigma_p$  = stress of a flat sheet
- $\bar{\sigma}^{(e)}, \bar{\sigma}^{(b)}$  = applied to the crack stress components
- $\sigma_x^{(e)}, \sigma_y^{(e)}, \tau_{xy}^{(e)}$  = stretching stress components
- $\sigma_x^{(b)}, \sigma_y^{(b)}, \tau_{xy}^{(b)}$  = bending stress components
- $\sigma_x, \sigma_y, \tau_{xy}$  = stresses as defined in text.

†Assistant Professor.

### INTRODUCTION

IT is well known that large, thin-walled pressure vessels resemble balloons and, like balloons, are subject to puncture and explosive loss. For any given material, under a specified stress field due to internal pressure, there will be a crack length in the material which will be self-propagating. Crack lengths less than the critical value will cause leakage but not destruction. However, if the critical length is ever reached, either by penetration or by the growth of a small fatigue crack, the explosion and complete loss of the structure occurs. The subject of eventual concern, therefore, is to assess analytically the relation between critical pressures and critical crack lengths in sheets which are initially curved.

The principal task, however, of fracture mechanics is precisely the prediction of such failure in the presence of sharp discontinuities, knowing only geometry, material behavior, etc. Specifically, the approach is based on a corollary of the First Law of Thermodynamics which was first applied to the phenomenon of fracture by Griffith[1]. His hypothesis was that the total energy of a cracked system subjected to loading remains constant as the crack extends an infinitesimal distance. It should, of course, be recognized that this is a necessary condition for failure but not sufficient.

Griffith applied his criterion to an infinite isotropic plate—under stretching—containing a flat, sharp-ended crack of length  $2c$  and has shown that it can be expressed in terms of an integral over the entire surface of the plate. Subsequently, Sanders[2] has proven that this integral is independent of the path; i.e. one may integrate along any simple contour enclosing the crack.

The purpose of this paper, therefore, is to extend Griffith's analysis and thus derive a fracture criterion applicable also to thin, shallow, initially curved sheets.

#### *Fracture criterion*

In deriving a fracture criterion, two ingredients are required: (1) the stress distribution due to the presence of the crack and (2) an energy balance for crack initiation. Because, however, the stress distribution currently available in the literature[3-6] for initially curved sheets is valid only in the immediate vicinity of the crack tip, we proceed to derive a criterion using only the singular part of the stresses and integrating over the area enclosed by the contour  $\Gamma$  (see Fig. 1) and through the thickness. Inasmuch as the contour  $\Gamma$  is a non-simple smooth curve, Sanders' conclusion can not be applied and the criterion, therefore, is approximate.

In view of the above, the total energy of that portion of the initially curved sheet

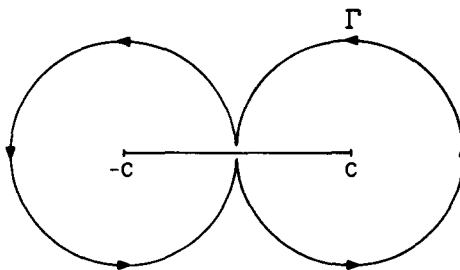


Fig. 1. Path  $\Gamma$  of the energy integral.

enclosed by that surface area, whose projection on the base plane is  $\Gamma$ , is given by

$$U_{\text{system}} = U_0 + \gamma^*(2A + Ph) + 4\gamma^*ch - 2\frac{c}{8G} \int_{-h/2}^{h/2} \int_0^c \int_{-\pi}^{\pi} \left\{ \frac{1-\nu}{1+\nu} (\sigma_x + \sigma_y)^2 + (\sigma_x - \sigma_y)^2 + (2\tau_{xy})^2 \right\} r \, dr \, d\theta \, dz \quad (1)$$

where the stresses  $\sigma_x$ ,  $\sigma_y$ ,  $\tau_{xy}$  are given in [3-6] as the sum of the extensional and bending stress components, i.e.

$$\sigma_x = \sigma_x^{(e)} + \sigma_x^{(b)} \quad (2)$$

$$\sigma_y = \sigma_y^{(e)} + \sigma_y^{(b)} \quad (3)$$

$$\tau_{xy} = \tau_{xy}^{(e)} + \tau_{xy}^{(b)} \quad (4)$$

with

$$\sigma_x^{(e)} = P^{(e)}\sqrt{(c/2r)} \left( \frac{3}{4} \cos \frac{\theta}{2} + \frac{1}{4} \cos \frac{5\theta}{2} \right) + 0(r^0) \quad (5)$$

$$\sigma_y^{(e)} = P^{(e)}\sqrt{(c/2r)} \left( \frac{5}{4} \cos \frac{\theta}{2} - \frac{1}{4} \cos \frac{5\theta}{2} \right) + 0(r^0) \quad (6)$$

$$\tau_{xy}^{(e)} = P^{(e)}\sqrt{(c/2r)} \left( -\frac{1}{4} \sin \frac{\theta}{2} + \frac{1}{4} \sin \frac{5\theta}{2} \right) + 0(r^0) \quad (7)$$

and

$$\sigma_x^{(b)} = P^{(b)}\frac{z}{h}\sqrt{(c/2r)} \left( -\frac{3-3\nu}{4} \cos \frac{\theta}{2} - \frac{1-\nu}{4} \cos \frac{5\theta}{2} \right) + 0(r^0) \quad (8)$$

$$\sigma_y^{(b)} = P^{(b)}\frac{z}{h}\sqrt{(c/2r)} \left( \frac{11+5\nu}{4} \cos \frac{\theta}{2} + \frac{1-\nu}{4} \cos \frac{5\theta}{2} \right) + 0(r^0) \quad (9)$$

$$\tau_{xy}^{(b)} = P^{(b)}\frac{z}{h}\sqrt{(c/2r)} \left( -\frac{7+\nu}{4} \sin \frac{\theta}{2} - \frac{1-\nu}{4} \sin \frac{5\theta}{2} \right) + 0(r^0). \quad (10)$$

The stress coefficients  $P^{(e)}$  and  $P^{(b)}$  are functions of the geometry of the shell and can be found in the Appendix.

Upon substituting (2-10) into (1) and integrating, one has

$$U_{\text{system}} = U_0 + \gamma^*(2A + Ph) + 4\gamma^*ch - \frac{2c^2\pi h}{8G} \left\{ \frac{33+6\nu-7\nu^2}{6} [P^{(b)}]^2 + \frac{9-7\nu}{2(1+\nu)} [P^{(e)}]^2 \right\}. \quad (11)$$

Thus, following Griffith's hypothesis, for crack instability, one requires

$$\frac{\partial U_{\text{system}}}{\partial c} = 0 \quad (12)$$

or

$$\frac{(33+6\nu-7\nu^2)(1+\nu)}{3(9-7\nu)} \left[ P^{(b)} \right]^2 + \left[ P^{(e)} \right]^2 = \frac{16G\gamma^*}{c\pi} \cdot \frac{2(1+\nu)}{9-7\nu} \equiv (\sigma_F)^2 \quad (13)$$

which in the case of flat sheets reduces to

$$\frac{(33+6\nu-7\nu^2)(1+\nu)}{3(9-7\nu)(4-\nu_0)^2} \left[ \bar{\sigma}^{(b)} \right]^2 + \left[ \bar{\sigma}^{(e)} \right]^2 = \frac{16G\gamma^*}{c\pi} \cdot \frac{2(1+\nu)}{9-7\nu}. \quad (14)$$

In general, the geometrical character of (13) is a family of ellipses whose semi-major and semi-minor axes are

$$\frac{\sqrt{3(9-7\nu)}(4-\nu_0)}{\sqrt{1+\nu}\sqrt{33+6\nu-7\nu^2}} \sigma_F, \sigma_F$$

respectively.

It is of some practical value to be able to correlate flat sheet behavior with that of initially curved specimens. In experimental work on brittle fracture for example, considerable time might be saved if one could predict the response behavior of curved sheets from flat sheet test data. In answering this question, one may combine (13) and (14) and for  $\bar{\sigma}^{(b)} = 0$  we obtain

$$\frac{\bar{\sigma}_{\text{shell}}^{(e)}}{\bar{\sigma}_{\text{plate}}^{(e)}} = \frac{1}{\left\{ \frac{(33+6\nu-7\nu^2)(1+\nu)}{3(9-7\nu)} J^2 + I^2 \right\}^{1/2}} \quad (15)$$

In particular, if one specializes (15) to an axial crack in a cylindrical pressure vessel, one has

$$\frac{\sigma_h}{\sigma_p} = \frac{1}{\left\{ \frac{(33+6\nu-7\nu^2)(1+\nu)}{3(9-7\nu)} J_{c,a}^2 + I_{c,a}^2 \right\}^{1/2}} \quad (16)$$

which for  $\lambda < 1$  simplifies to

$$\frac{\sigma_h}{\sigma_p} \approx \frac{1}{\sqrt{1+0.49\lambda^2}}. \quad (16a)$$

In judging the adequacy of a theory, one often compares theoretical and experimental results; therefore, in Fig. 2, we compare our results with the experimental data obtained by Kihara, Ikeda and Iwanaga [7] on cylindrical pipes containing axial notches. The reader will note that the predicted theoretical values are somewhat conservative and compare fairly well with the experimental data. One is led, therefore, to believe that (15) can be used to predict response behavior of curved sheets from flat sheet test data.

As a consequence of (13), it is also possible to obtain a relation between the critical crack length in a shell and the critical crack length in a plate in terms of their corresponding loadings, in particular

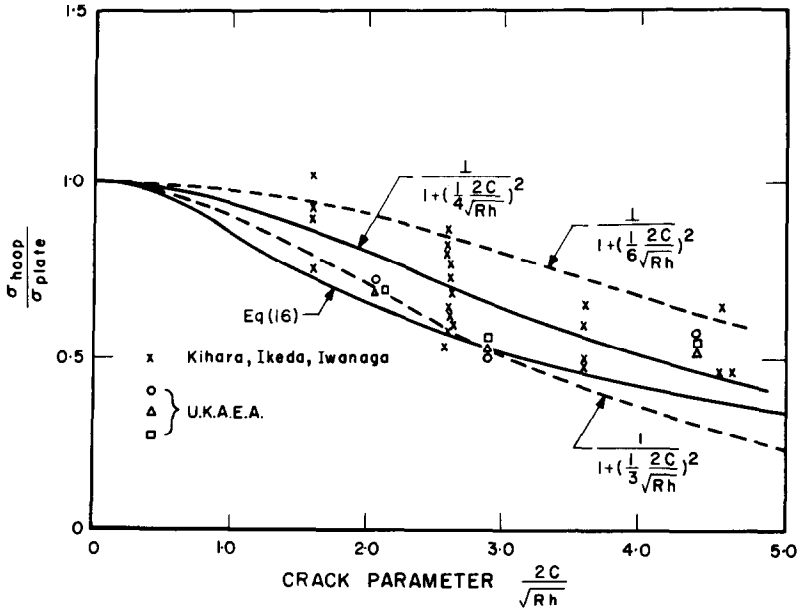


Fig. 2. Correlation between fracture stress ratio of pipe and flat plate and  $(2c/\sqrt{Rh})$ .

$$\left(\frac{l_{shell}}{l_{plate}}\right)_{critical} \approx \frac{\{[P^{(e)}]^2 + \delta[P^{(b)}]^2\}_{plate}}{\{[P^{(e)}]^2 + \delta[P^{(b)}]^2\}_{shell}} \tag{17}$$

where the constant  $\delta$  is defined as

$$\delta \equiv \frac{(33 + 6\nu - 7\nu^2)(1 + \nu)}{3(9 - 7\nu)}$$

As a practical matter, if one considers the same 'applied loadings'† on the shell and on the plate, i.e.  $(\bar{\sigma}^{(b)})_{plate} = (\bar{\sigma}^{(b)})_{shell} = 0$  and  $(\bar{\sigma}^{(e)})_p = (\bar{\sigma}^{(e)})_{shell} = \bar{\sigma}^{(e)}$ , then (17) reduces to

$$\left(\frac{l_{shell}}{l_{plate}}\right)_{critical} \approx \frac{1}{\left(\frac{P_{shell}^{(e)}}{P_{plate}^{(e)}}\right)^2} \tag{17a}$$

where the right hand side is a function of the geometry of the shell, its crack length and its material properties. In general, this quantity is less than unity, which suggests that shells present a reduced resistance to fracture initiation that is basically of geometric origin. For  $\lambda = 1$ , an axial crack in a pressurized cylindrical vessel gives

$$\left(\frac{l_{shell}}{l_{plate}}\right)_{critical} \approx \frac{1}{1 + \frac{5\pi\lambda^2}{32}} \Big|_{\lambda=1} \approx 0.67. \tag{17b}$$

†For a definition of  $\bar{\sigma}^{(e)}$  and  $\bar{\sigma}^{(b)}$ , see Appendix.

*Plasticity correction*

Due to the presence of high stresses in the vicinity of the crack tip, when the appropriate yield criterion is satisfied then localized, plastic deformation occurs and a plastic zone is created. This phenomenon effectively increases the crack length and therefore must be accounted for. Following Dugdale[8], the plastic zone size (see Fig. 3) is determined by the relation

$$\frac{c}{c_e} = \cos\left(\frac{\pi \sigma}{2\sigma_y}\right) \tag{18}$$

or

$$\frac{\rho}{c} = \sec\left(\frac{\pi \sigma}{2\sigma_y}\right) - 1. \tag{19}$$

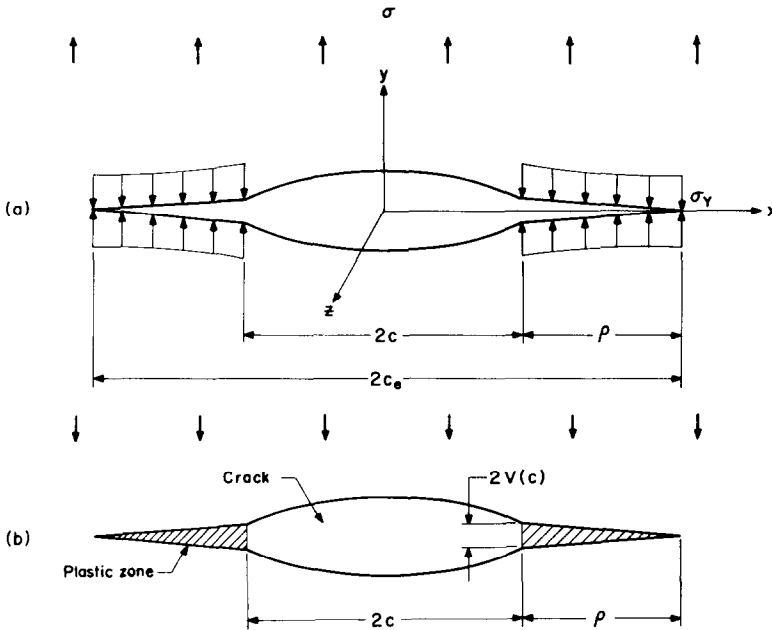


Fig. 3. (a) Internal stress distribution used in the Dugdale model of elastic-plastic deformation near a crack of length  $2c$  under plane-stress tensile loading. (b) Displacements  $2V$  associated with crack opening. After Hahn and Rosenfield[10].

This relation applies only to a perfect elastic-plastic behavior of a non strain-hardening material. McClintock[9], however, has suggested that a strain hardening material may be approximated by an ideally plastic one, if a stress higher than  $\sigma_y$  and lower than  $\sigma_u$  is chosen. Subsequently, Hahn and Rosenfield[10] suggested that  $\sigma_y$  in (17) be replaced by  $\sigma^* = (\sigma_u + \sigma_y)/2$ . Thus, correcting the Griffith–Irwin equation so as to include yielding and geometry effects, one has†

†For derivation, see [11]. A more sophisticated approach would be to treat  $\sigma^*$  and  $K$  as constants to be determined such that (20) presents 'a best fit'. One may, however, choose for  $\sigma^*$  the value suggested by Hahn and Rosenfield or the alternate value suggested by the author:

$$\frac{\sigma_y + \frac{\sigma_y + \sigma_u}{2}}{2}$$

$$\sigma_F = \frac{2\sigma^*}{\pi} \cos^{-1} \left[ \exp \left( -\frac{\pi K^2}{8\sigma^{*2}c} \right) \right] \quad (20)$$

which upon substituting for  $\sigma_F$  from (13) one has

$$\sigma^{(e)} \left\{ \frac{(33 + 6\nu - 7\nu^2)(1 + \nu)}{3(9 - 7\nu)} J^2 + I^2 \right\}^{1/2} = \frac{2\sigma^*}{\pi} \cos^{-1} \left[ \exp \left( -\frac{\pi K^2}{8\sigma^{*2}c} \right) \right]. \quad (21)$$

It should be emphasized that this criterion is not valid after general yield. At the present time, there are not adequate criteria to handle these problems. Furthermore, inasmuch as a Dugdale model was used, it is only natural, therefore, to consider uniaxial yielding too. For small values of  $\sigma_F$ , i.e. for  $\sigma_F < 0.6\sigma_y$ , (21) may be approximated by the simpler form

$$\sigma^{(e)} \left\{ \frac{(33 + 6\nu - 7\nu^2)(1 + \nu)}{3(9 - 7\nu)} J^2 + I^2 \right\}^{1/2} = \frac{K}{\sqrt{\pi c}}. \quad (22)$$

Specializing now (21) to a cylindrical pressure vessel containing an axial crack, one finds

$$\sigma_h I_{c,a} = \frac{2\sigma^*}{\pi} \cos^{-1} \left[ \exp \left( -\frac{\pi K^2}{8\sigma^{*2}c} \right) \right] \quad (23a)$$

which for  $\lambda < 1$  can be written as

$$\sigma_h \left\{ 1 + \frac{5\pi}{64} \lambda^2 \right\} \approx \frac{2\sigma^*}{\pi} \cos^{-1} \left[ \exp \left( -\frac{\pi K^2}{8\sigma^{*2}c} \right) \right]. \quad (23b)$$

By (23a) one would expect, therefore, to predict failure in cylindrical pressure vessels containing axial cracks. Inasmuch as theory in general is not useful unless there exists experimental evidence to support it, we compare our results with a set of data obtained by Anderson and Sullivan[12] for 6 in. dia. 0.060 in. thick cylinders of 2014-T6 aluminum tested at  $-320^\circ\text{F}$ . In order to utilize (23a), one must know *a priori* the fracture toughness  $K$ . This can be accomplished in the following manner: (1) use the test data and compute the  $K$ 's, (2) find the average  $K$ , and (3) use the  $K_{av}$  to predict failing hoop pressures. The results are given in Table 1 and are plotted in Fig. 4.

As the reader can see, the agreement between theory and experiment is fairly good. It should, however, be pointed out that if one disregards the first two points, on the basis that they are too close to the yield point, and compute the  $K_{av}$  from the rest of the data, the agreement will be even better.

Finally, specializing (21) to a spherical shell, one has

$$\sigma_h [I_s] = \frac{2\sigma^*}{\pi} \cos^{-1} \left[ \exp \left( -\frac{\pi K^2}{8c\sigma^{*2}} \right) \right] \quad (24a)$$

and for  $\lambda < 1$ , one may use its asymptotic form

$$\sigma_h \left\{ 1 + \frac{3\pi\lambda^2}{32} \right\} = \frac{2\sigma^*}{\pi} \cos^{-1} \left[ \exp \left( -\frac{\pi K^2}{8\sigma^{*2}c} \right) \right]. \quad (24b)$$

Table 1†. Aluminum 2014 T6. Material: 2014-T6 aluminum at  $-320^{\circ}\text{F}$ ,  
 $\sigma_u = 84 \text{ kpsi}$   $\sigma_y = 72 \text{ kpsi}$

c	$\lambda$	$\sigma_h$ calc. ksi	$\sigma_h$ calc. ksi	$\sigma_h$ exp ksi
		using $K = 50.2 \text{ ksi}\sqrt{\text{in}}$ $\sigma^* = 78 \text{ ksi}$	using $K = 52.3 \text{ ksi}\sqrt{\text{in}}$ $\sigma^* = 75 \text{ ksi}$	
0.056	0.24	73.5	71.5	71.6
0.075	0.32	70.2	69.4	70.6
0.100	0.43	65.0	64.5	63.7
0.125	0.53	60.5	60.8	58.5
0.150	0.64	55.5	56.5	52.2
0.200	0.85	48.0	48.8	47.4
0.250	1.06	41.3	42.3	40.1
0.375	1.60	29.7	30.6	30.2
0.500	2.13	22.9	23.4	23.1
0.625	2.66	17.8	18.3	18.6
0.875	3.72	11.9	12.2	14.4
1.000	4.25	10.1	10.4	11.3

†Note:  $\sigma^* = [(\sigma_u + \sigma_y)/2] = 78 \text{ ksi}$  and  $\sigma^* = [(\sigma_y + (\sigma_u + \sigma_y)/2)]/2 = 75 \text{ ksi}$ .

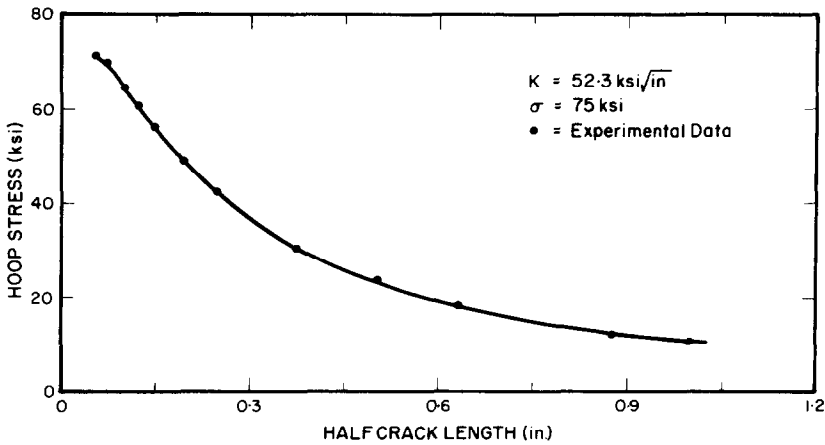


Fig. 4. Comparison between theory and experiment for 2014-T6 aluminum cylindrical vessels.

A comparison between the theoretical and experimental data obtained by Sopher *et al.*[13] for 9 in. dia.,  $\frac{3}{4}$  in. thickness spheres with through cracks is given by Table 2 and Fig. 5. The comparison, as the reader can see, is very good.†

In conclusion, therefore, one may use (21) to predict failures in pressurized vessels knowing only geometry, ultimate stress, yield stress, crack length and fracture toughness. The applications of such a relation are numerous. In the space industry, for example, where weight is a critical parameter, this relation will enable the engineer to design light and strong structures capable of carrying the necessary loads without failure to occur.

†For further comparisons see the author's paper "On the Prediction of Failure in Pressurized Vessels" presented at the First International Conference on Pressure Vessel Technology at Delft, the Netherlands, Sept. 29–Oct. 2, 1969 (ASME).

Table 2†. Material: ABS-B steel at 40°F  $\sigma_u = 59.4$  ksi,  $\sigma_y = 30.7$  ksi

$c$	$\lambda$	$\sigma_h$ calc. ksi	$\sigma_h$ calc. ksi	$\sigma_h$ exp. ksi
		using $K = 102 \text{ ksi}\sqrt{\text{in}}$ $\sigma^* = 37.9 \text{ ksi}$	using $K = 95.8 \text{ ksi}\sqrt{\text{in}}$ $\sigma^* = 45 \text{ ksi}$	
2	0.57	28.4	29.2	28.15
2	0.57	28.4	29.2	28.15
4	1.14	19.8	19.5	19.70
5	1.42	16.8	16.2	16.90
6	1.70	14.0	13.6	13.10
8	2.27	10.3	10.0	11.20

†Note:  $\sigma^* = [(\sigma_y + \sigma_u)/2] = 45$  ksi and  $\sigma\& = [(\sigma_y + (\sigma_y + \sigma_u)/2)/2] = 37.9$  ksi.

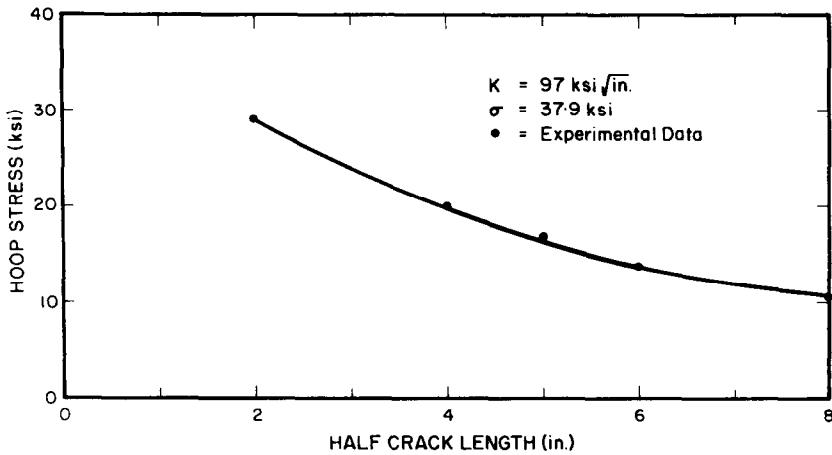


Fig. 5. Comparison between theory and experiment for ABS-B steel spherical vessels.

Table 3. Defines the coefficients  $I$  and  $J$  in (21) for two types of geometries: a cylindrical and spherical shell

		For all $\lambda \leq 8$	For $\lambda < 1$
<p>Long cylinder axial crack</p>		$I = I_{c,a}$ from Fig. 6 or Table 4	$I_{c,a} \approx 1 + \frac{5\pi}{64} \lambda^2$
		$J = J_{c,a}$ from Fig. 7 or Table 4	$J_{c,a} \approx 0$
		For all $\lambda \leq 8$	For $\lambda < 1$
<p>Long cylinder peripheral crack</p>		$I = I_{c,p}$ from Fig. 8	$I_{c,p} \approx 1 + \frac{\pi \lambda^2}{64}$
		$J = J_{c,p}$ from Fig. 8	$J_{c,p} \approx 0$
		For all $\lambda \leq 5.5$	For $\lambda < 1$
<p>Spherical cap</p>		$I = I_s$ from Fig. 9 or Table 4	$I_s \approx 1 + \frac{3\pi \lambda^2}{32}$
		$J = J_s$ from Fig. 10 or Table 4	$J_s \approx 0$

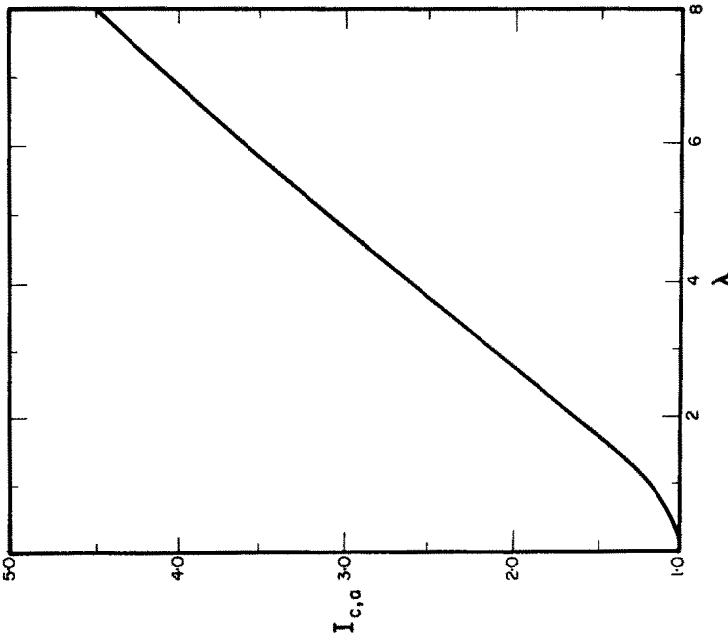


Fig. 6. Stress singularities for a cylindrical shell containing an axial crack [14].

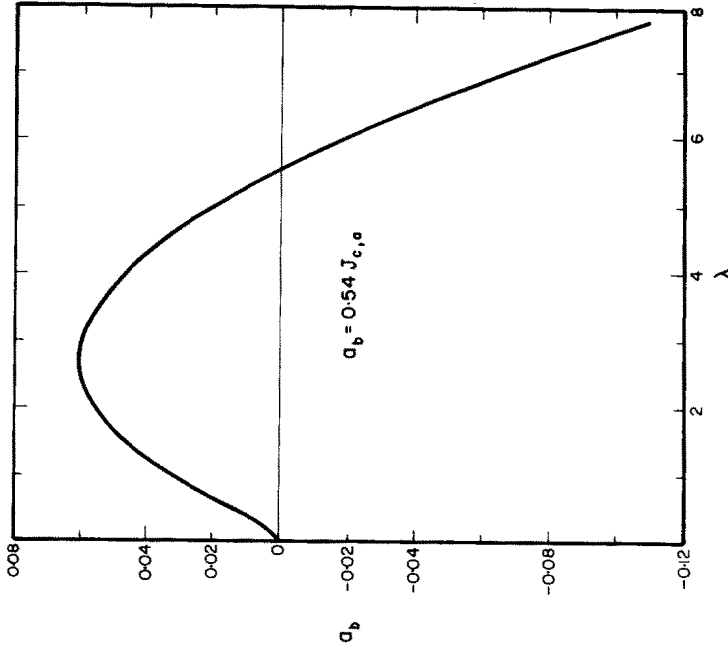


Fig. 7. Stress singularities for a cylindrical shell containing an axial crack [14].

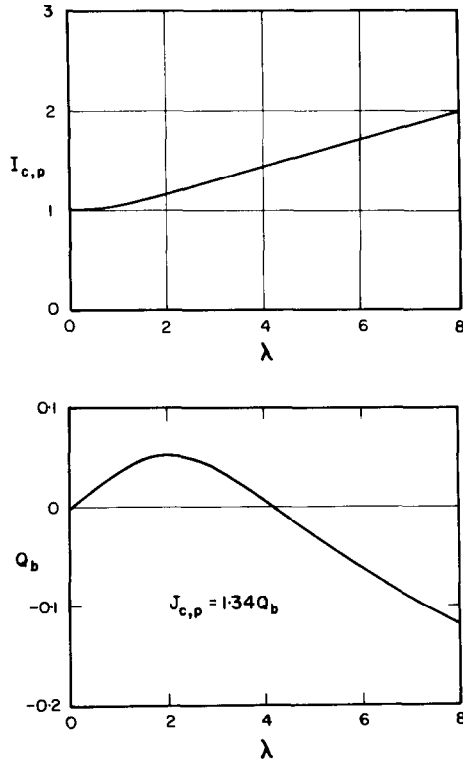


Fig. 8. Stress singularities for a cylindrical shell containing a peripheral crack [15].

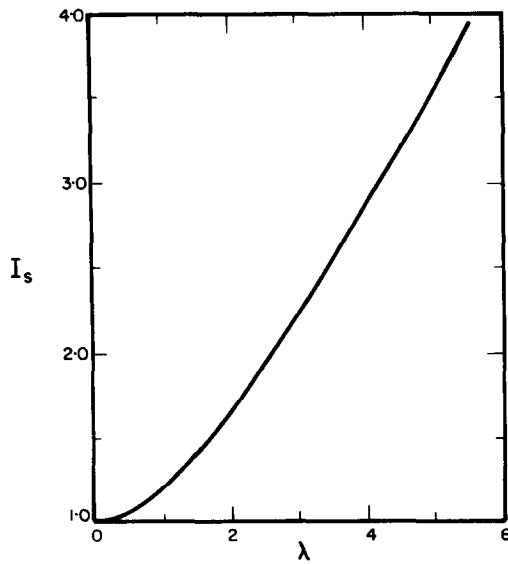


Fig. 9. Stress singularity for a spherical shell containing a crack [14].

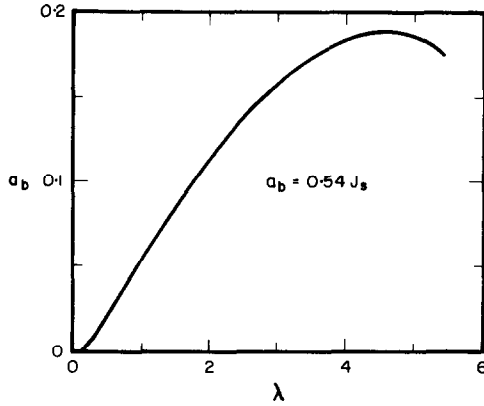


Fig. 10. Stress singularity for a spherical shell containing a crack [14].

Table 4. Stress coefficients

$\lambda$	Cylinder (axial)		Sphere	
	$A_p = I_{c,a}$	$a_b = 0.54 J_{c,a}$	$A_e = I_s$	$a_b = 0.54 J_c$
0.2	1.0096	0.00410	1.0112	0.00611
0.4	1.0371	0.01124	1.0422	0.01693
0.6	1.0795	0.01902	1.0887	0.02919
0.8	1.1344	0.02659	1.1479	0.04186
1.0	1.1993	0.03359	1.2174	0.05448
1.2	1.2723	0.03985	1.2956	0.06685
1.4	1.3519	0.04529	1.3812	0.07886
1.6	1.4367	0.04990	1.4731	0.09045
1.8	1.5256	0.05368	1.5706	0.10155
2.0	1.6177	0.05664	1.6729	0.11216
2.2	1.7122	0.05883	1.7795	0.12223
2.4	1.8085	0.06018	1.8899	0.13172
2.6	1.9060	0.06090	2.0038	0.14058
2.8	2.0045	0.06083	2.1208	0.14879
3.0	2.1035	0.06014	2.2408	0.15630
3.25	2.2276	0.05832	2.3947	0.16463
3.50	2.3519	0.05549	2.5526	0.17172
3.75	2.4761	0.05172	2.7143	0.17751
4.00	2.5999	0.04700	2.8796	0.18194
4.25	2.7232	0.04154	3.0485	0.18483
4.50	2.8459	0.03512	3.2208	0.18644
5.00	3.0895	0.02012	3.5750	0.18493
5.50	3.3303	0.00234	3.9446	0.17802
6.00	3.5681	0.02222		
6.50	3.8029	0.04130		
7.00	4.0347	0.06622		
7.50	4.2637	0.09350		
8.00	4.4895	0.12279		

*Acknowledgement*—This work was supported in part by the National Science Foundation, Grant no. GK-1440.

### REFERENCES

- [1] A. A. Griffith, The phenomena of rupture and flow in solids. *Trans. R. Soc. Lond.* **221**, (1920).
- [2] J. L. Sanders, On the Griffith–Irwin fracture theory. *Trans. ASME Series E* (1960).
- [3] E. S. Folias, *J. Math. Phys.* **44**, 164–176 (1965).
- [4] E. S. Folias, *Int. J. fracture Mech.* **1**, 104–113 (1965).
- [5] E. S. Folias, *Int. J. fracture Mech.* **3**, 1, 1–11 (1967).
- [6] E. S. Folias, *Int. J. fracture Mech.* **1**, 20–46 (1965).
- [7] H. Kihara, K. Ikeda and H. Iwanaga, Brittle fracture initiation of line pipe. Document No. X-371-66 *Int. Inst. Welding* (1966).
- [8] D. S. Dugdale, *J. Mech. Phys. Solids* **8**, 100 (1960).
- [9] F. A. McClintock, On notch sensitivity. *Weld. J. Res. Suppl.* **26**, 202 (1961).
- [10] G. T. Hahn and A. R. Rosenfield, Local yielding and extension of a crack under plane stress. *Acta Met.* **13** (1965).
- [11] A. S. Tetelman and A. J. McEvily, Jr., *Fracture of Structural Materials*, pp. 62–79. Wiley, New York (1967).
- [12] R. B. Anderson and T. L. Sullivan, Fracture mechanics of through cracked cylindrical pressure vessels. *NASA Tech. Note* No. 0-3252.
- [13] R. P. Sopher, A. L. Lowe, D. C. Martin and P. J. Tieppel, Evaluation of weld joint flaws as initiating points of brittle fracture. *Weld. J. Res.* **24**, 4415 (1959).
- [14] F. Erdogan and J. Kibler, Cylindrical and spherical shells with cracks. Submitted for publication to the *Int. J. fracture Mech.*
- [15] M. E. Duncan, A circumferential crack. Private communication.

(Received 26 November 1968)

### APPENDIX

The stress coefficients  $P^{(e)}$  and  $P^{(b)}$  for various shell geometries and for  $\lambda < 1$  are given in [3–6] as:

---

Sphere;  
for clamped  
spherical cap

$$P_s^{(e)} = \bar{\sigma}^{(e)} \left\{ 1 + \frac{3\pi}{32} \lambda^2 \right\} + \bar{\sigma}^{(b)} \frac{\sqrt{1-\nu^2\lambda^2}}{\sqrt{3(4-\nu_0)}} \left\{ \frac{7}{32} + \frac{3}{8} \left( \gamma + \ln \frac{\lambda}{4} \right) \right\}$$

$$\begin{aligned} \sigma^{(e)} &= qR/(2h) \\ \sigma^{(b)} &= 0 \end{aligned} \quad P_s^{(b)} = -\bar{\sigma}^{(e)} \frac{\sqrt{3}\lambda^2}{\sqrt{1-\nu^2(4-\nu_0)}} \left\{ \frac{8-7\nu_0}{32} + \frac{4-3\nu_0}{8} \left( \gamma + \ln \frac{\lambda}{4} \right) \right\} \\ - \frac{\bar{\sigma}^{(b)}}{4-\nu_0} \left\{ 1 + \frac{4-3\nu_0}{4-\nu_0} \frac{\pi\lambda^2}{32} \right\}$$


---

Flat plate

$$P_p^{(e)} = \bar{\sigma}^{(e)}$$

$$P_p^{(b)} = -\frac{\bar{\sigma}^{(b)}}{4-\nu_0}$$


---

Cylinder,  
axial;  
for long  
cylinder

$$P_{c.a}^{(e)} = \bar{\sigma}^{(e)} \left\{ 1 + \frac{5\pi}{64} \lambda^2 \right\} + \bar{\sigma}^{(b)} \frac{\sqrt{1-\nu^2\lambda^2}}{\sqrt{3(4-\nu_0)}} \left\{ \frac{42-37\nu_0}{96\nu_0} + \frac{6-5\nu_0}{16\nu_0} \left( \gamma + \ln \frac{\lambda}{8} \right) \right\}$$

$$\begin{aligned}\bar{\sigma}^{(e)} &= qR/h \\ \bar{\sigma}^{(b)} &= 0\end{aligned}$$

$$\begin{aligned}P_{c,a}^{(b)} &= -\bar{\sigma}^{(e)} \frac{\sqrt{3}\lambda^2}{\sqrt{1-\nu^2}(4-\nu_0)} \left\{ \frac{42-37\nu_0}{96} + \frac{6-5\nu_0}{16} \left( \gamma + \ln \frac{\lambda}{8} \right) \right\} \\ &\quad - \frac{\bar{\sigma}^{(b)}}{4-\nu_0} \left\{ 1 + \frac{12\nu_0-5\nu_0^2-8\pi\lambda^2}{(4-\nu_0)\nu_0} \frac{\pi\lambda^2}{64} \right\}\end{aligned}$$


---

Cylinder,  
peripheral;  
for long  
cylinder

$$P_{c,\nu}^{(e)} = \bar{\sigma}^{(e)} \left\{ 1 + \frac{\pi\lambda^2}{64} \right\} + \bar{\sigma}^{(b)} \frac{\sqrt{1-\nu^2}\lambda^2}{\sqrt{3}(4-\nu_0)} \left\{ \frac{1+\nu}{32\nu_0} \left( 1 + 2\gamma + 2 \ln \frac{\lambda}{8} \right) \right\}$$

$$\begin{aligned}\bar{\sigma}^{(e)} &= qR/(2h) \\ \bar{\sigma}^{(b)} &= 0\end{aligned}$$

$$\begin{aligned}P_{c,\nu}^{(b)} &= -\bar{\sigma}^{(e)} \frac{\sqrt{3}\lambda^2}{\sqrt{1-\nu^2}(4-\nu_0)} \left\{ \frac{1+\nu}{32} \left( 1 + 2\gamma + 2 \ln \frac{\lambda}{8} \right) \right\} \\ &\quad - \frac{\bar{\sigma}^{(b)}}{4-\nu_0} \left\{ 1 - \frac{5+2\nu+\nu^2}{(4-\nu_0)\nu_0} \frac{\pi\lambda^2}{64} \right\}\end{aligned}$$


---

For  $\lambda \geq 1$ , the stress coefficients for  $\bar{\sigma}^{(b)} = 0$  are given by:

Sphere [14]  $P_s^{(e)} = \bar{\sigma}^{(e)} I_s$  (see Table 4 or Fig. 9)

$$P_s^{(b)} = \bar{\sigma}^{(e)} J_s \text{ (see Table 4 or Fig. 10)}$$


---

Cylinder  
axial [14]

$$P_{c,a}^{(e)} = \bar{\sigma}^{(e)} I_{c,a} \text{ (see Table 4 or Fig. 6)}$$

$$P_{c,a}^{(b)} = \bar{\sigma}^{(e)} J_{c,a} \text{ (see Table 4 or Fig. 7)}$$


---

Cylinder,  
peripheral [15]

$$P_{c,\nu}^{(e)} = \bar{\sigma}^{(e)} I_{c,\nu} \text{ (see Fig. 8)}$$

$$P_{c,\nu}^{(b)} = \bar{\sigma}^{(e)} J_{c,\nu} \text{ (see Fig. 8)}$$


---

**Résumé**—A la suite de Griffith, un critère de rupture est dérivé, incorporant une correction de géométrie et de plasticité et permettant de prédire toute défautuosité dans les cuves pressurisées. Une comparaison, qui s'avère très bonne, a été effectuée entre quelques séries de données expérimentales prises au hasard.

**Zusammenfassung**—Für die Vorhersage von Rissen in einem Druckbehälter wird nach Griffith ein Bruchkriterium abgeleitet, das eine Geometrie-sowie eine Plastizitätskorrektur enthält. Der Vergleich mit einigen, willkürlich gewählten Gruppen von Versuchsergebnissen ist sehr befriedigend.